Article

[FeFe]-Hydrogenase-Catalyzed H Production in a Photoelectrochemical Biofuel Cell

Michael Hambourger, Miguel Gervaldo, Drazenka Svedruzic, Paul W. King, Devens Gust, Maria Ghirardi, Ana L. Moore, and Thomas A. Moore

J. Am. Chem. Soc., **2008**, 130 (6), 2015-2022 • DOI: 10.1021/ja077691k

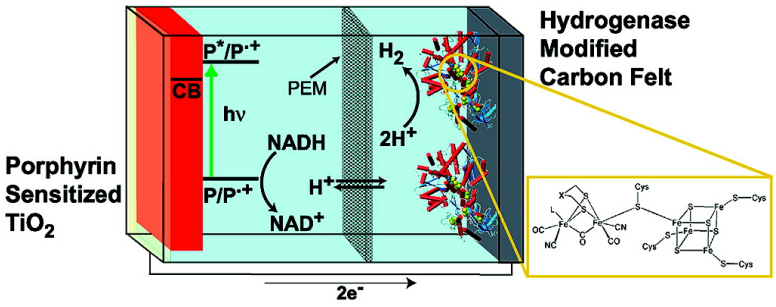

More About This Article

Additional resources and features associated with this article are available within the HTML version:

- Supporting Information
- Links to the 5 articles that cite this article, as of the time of this article download
- Access to high resolution figures
- Links to articles and content related to this article
- Copyright permission to reproduce figures and/or text from this article

View the Full Text HTML

J|A|C|S
ARTICLES
Published on Web 01/19/2008

[FeFe]-Hydrogenase-Catalyzed H_2 Production in a Photoelectrochemical Biofuel Cell

Michael Hambourger,[†] Miguel Gervaldo,[†] Drazenka Svedruzic,[‡] Paul W. King,*[,‡] Devens Gust,*[,†] Maria Ghirardi,*[,‡] Ana L. Moore,*[,†] and Thomas A. Moore*[,†]

Center for Bioenergy and Photosynthesis and Department of Chemistry and Biochemistry, Arizona State University, Tempe, Arizona 85287-1604, and Chemical and Biosciences Center, National Renewable Energy Laboratory, Golden, Colorado 80401

Received October 5, 2007; E-mail: tmoore@asu.edu

Abstract: The *Clostridium acetobutylicum* [FeFe]-hydrogenase HydA has been investigated as a hydrogen production catalyst in a photoelectrochemical biofuel cell. Hydrogenase was adsorbed to pyrolytic graphite edge and carbon felt electrodes. Cyclic voltammograms of the immobilized hydrogenase films reveal cathodic proton reduction and anodic hydrogen oxidation, with a catalytic bias toward hydrogen evolution. When corrected for the electrochemically active surface area, the cathodic current densities are similar for both carbon electrodes, and ~40% of those obtained with a platinum electrode. The high surface area carbon felt/hydrogenase electrode was subsequently used as the cathode in a photoelectrochemical biofuel cell. Under illumination, this device is able to oxidize a biofuel substrate and reduce protons to hydrogen. Similar photocurrents and hydrogen production rates were observed in the photoelectrochemical biofuel cell using either hydrogenase or platinum cathodes.

Introduction

The conversion of solar energy to stored chemical energy is one promising means of providing for long-term energy needs. Systems for the direct solar production of fuels essentially mimic the natural processes of photosynthesis.[1−3] Photon absorption is used to generate a charge separated state, which must be efficiently coupled to catalytic centers.[4,5] Hydrogen is an appealing energy carrier[6] because of the closed redox loop between water, H_2, and O_2.

Hydrogenases catalyze the reversible reaction $2H^+ + 2e^- \rightleftarrows H_2$ using base metals, predominantly nickel and iron, at their catalytic sites.[7−11] As a result, there is interest in using hydrogenases as replacements for platinum in hydrogen production systems and hydrogen fuel cells.[12,13] The technique of protein film voltammetry[14] allows the rate of direct electron transfers between adsorbed enzyme and an electrode to be studied as a function of the driving force. For hydrogenase-modified electrodes, cyclic voltammograms reflect the amount and orientation of hydrogenase at the electrode surface, the availability of H^+ and H_2, the rate of interfacial electron transfers, and inherent properties of the enzyme.[15] Direct electron transfers with an electrode have been well characterized for the [NiFe]-hydrogenases,[16−21] which exhibit a catalytic bias toward hydrogen oxidation, using this method.[22,23] A handful of reports describe electrochemical studies of [FeFe]-hydrogenases.[23−26] In the hydrogen oxidation reaction, [NiFe]-hydrogenase electrodes have compared favorably to platinum electrodes.[27] In terms of photochemical hydrogen generation, the [FeFe]-

[†] Arizona State University.
[‡] National Renewable Energy Laboratory.

(1) Gust, D.; Moore, T. A.; Moore, A. L. *Acc. Chem. Res.* **2001**, *34*, 40−48.
(2) Kruse, O.; Rupprecht, J.; Mussgnug, J. H.; Dismukes, G. C.; Hankamer, B. *Photochem. Photobiol. Sci.* **2005**, *4*, 957−969.
(3) LaVan, D. A.; Cha, J. N. *Proc. Natl. Acad. Sci. U.S.A.* **2006**, *103*, 5251−5255.
(4) Harriman, A. *Angew. Chem., Int. Ed.* **2004**, *43*, 4985−4987.
(5) Kamat, P. V. *J. Phys. Chem. C* **2007**, *111*, 2834−2860.
(6) Turner, J. A. *Science* **2004**, *305*, 972−974.
(7) Evans, D. J.; Pickett, C. J. *Chem. Soc. Rev.* **2003**, *32*, 268−275.
(8) Vignais, P. M.; Colbeau, A. *Curr. Issues Mol. Biol.* **2004**, *6*, 159−188.
(9) Armstrong, F. A. *Curr. Opin. Chem. Biol.* **2004**, *8*, 133−140.
(10) Volbeda, A.; Fontecilla-Camps, J. C. *Coord. Chem. Rev.* **2005**, *249*, 1609−1619.
(11) Nicolet, Y.; Cavazza, C.; Fontecilla-Camps, J. C. *J. Inorg. Biochem.* **2002**, *91*, 1−8.
(12) Karyakin, A. A.; Morozov, S. V.; Karyakina, E. E.; Zorin, N. A.; Perelygin, V. V.; Cosnier, S. *Biochem. Soc. Trans.* **2005**, *33*, 73−75.
(13) Vincent, K. A.; Cracknell, J. A.; Lenz, O.; Zebger, I.; Friedrich, B.; Armstrong, F. A. *Proc. Natl. Acad. Sci. U.S.A.* **2005**, *102*, 16951−16954.
(14) Armstrong, F. A.; Heering, H. A.; Hirst, J. *Chem. Soc. Rev.* **1997**, *26*, 169−179.
(15) Vincent, K. A.; Parkin, A.; Armstrong, F. A. *Chem. Rev.* **2007**, *107*, 4366−4413.
(16) Léger, C.; Jones, A. K.; Roseboom, W.; Albracht, S. P. J.; Armstrong, F. A. *Biochemistry* **2002**, *41*, 15736−15746.
(17) Léger, C.; Jones, A. K.; Albracht, S. P. J.; Armstrong, F. A. *J. Phys. Chem. B* **2002**, *106*, 13058−13063.
(18) Jones, A. K.; Lamle, S. E.; Pershad, H. R.; Vincent, K. A.; Albracht, S. P. J.; Armstrong, F. A. *J. Am. Chem. Soc.* **2003**, *125*, 8505−8514.
(19) Lojou, É.; Giudici-Orticoni, M.-T.; Bianco, P. *J. Electroanal. Chem.* **2005**, *577*, 79−86.
(20) Alonso-Lomillo, M. A.; Rüdiger, O.; Maroto-Valiente, A.; Velez, M.; Rodríguez-Ramos, I.; Muñoz, F. J.; Fernández, V. M.; De Lacey, A. L. *Nano Lett.* **2007**, *7*, 1603−1608.
(21) Léger, C.; Dementin, S.; Bertrand, P.; Rousset, M.; Guigliarelli, B. *J. Am. Chem. Soc.* **2004**, *126*, 12162−12172.
(22) Pershad, H. R.; Duff, J. L. C.; Heering, H. A.; Duin, E. C.; Albracht, S. P. J.; Armstrong, F. A. *Biochemistry* **1999**, *38*, 8992−8999.
(23) Vincent, K. A.; Parkin, A.; Lenz, O.; Albracht, S. P. J.; Fontecilla-Camps, J. C.; Cammack, R.; Friedrich, B.; Armstrong, F. A. *J. Am. Chem. Soc.* **2005**, *127*, 18179−18189.
(24) Parkin, A.; Cavazza, C.; Fontecilla-Camps, J. C.; Armstrong, F. A. *J. Am. Chem. Soc.* **2006**, *128*, 16808−16815.
(25) Butt, J. N.; Filipiak, M.; Hagen, W. R. *Eur. J. Biochem.* **1997**, *245*, 116−122.
(26) Guiral-Brugna, M.; Giudici-Orticoni, M. T.; Bruschi, M.; Bianco, P. *J. Electroanal. Chem.* **2001**, *510*, 136−143.

hydrogenases are appealing catalysts because of a catalytic activity greater than that of their [NiFe] analogues in the hydrogen evolution reaction.[23,28] Oxygen is a competitive inhibitor of both types of hydrogenase. Whereas most [FeFe]-hydrogenases are irreversibly damaged, inhibition of most [NiFe]-hydrogenases is reversible, and certain [NiFe]-hydrogenases are even oxygen-tolerant.[23,28,29] Members from both classes of hydrogenase have been shown to undergo anaerobic oxidative inactivation at anodic potentials, in certain cases affording improved O_2 tolerance.[18,23]

Both [NiFe] and [FeFe]-hydrogenases are reported to form adsorbed layers on many types of carbon,[20,25,26,30−34] most commonly on pyrolytic graphite edge (PGE) electrodes.[35] The variety of carbon electrodes used in the literature suggests that the nonspecific interaction between hydrogenase and carbon may be a general phenomenon, with some portion of the adsorbed enzyme binding in an orientation, and at a site, suitable for direct electron transfers with the electrode. Control over the orientation of adsorbed hydrogenases has also been demonstrated at a PGE electrode, resulting in higher current densities as compared to that of randomly oriented adsorbed hydrogenases.[36]

In the present study, a recombinantly produced HydA [FeFe]-hydrogenase from *Clostridium acetobutylicum* (*Ca*HydA) has been investigated as a catalyst for photoelectrochemical H_2 production. *Ca*HydA shares a high degree of sequence homology (70% identity)[37] with the *Clostridium pasteurianum* [FeFe]-hydrogenase CpI, for which structural data exist.[38] *Ca*HydA is a 65.4 kD protein composed of a highly conserved catalytic domain and an N-terminal accessory-cluster domain. The mature form of *Ca*HydA contains the catalytic [6Fe−6S] H-cluster and, based on homology to CpI, possesses an accessory-cluster domain that is predicted to contain one [2Fe−2S] and three [4Fe−4S] clusters. Surface-localized accessory clusters function to transfer electrons between external redox partners (i.e., ferredoxin, flavodoxin, or an electrode) and the buried catalytic H-cluster. Biochemical properties of the CpI type of clostridial [FeFe]-hydrogenase include high turnover numbers for the hydrogen evolution reaction and high solubilities.[39,40] *Ca*HydA was chosen for examination in the present work because of the ease of recombinant expression and the high catalytic activity for H_2 production.[37]

For this report, *Ca*HydA was initially studied electrochemically using PGE and carbon felt electrodes. For each electrode, immobilized *Ca*HydA films were characterized by cyclic voltammetry. The electrochemical responses provide insight into both the catalytic ability of *Ca*HydA and the interaction with the electrode. *Ca*HydA was studied at a PGE rotating disc electrode (RDE) under conditions well described in the literature.[15] With fast rotation, mass-transport effects can be minimized and the performance of adsorbed *Ca*HydA directly assessed. These data are compared to those obtained with a platinum RDE. *Ca*HydA was also studied electrochemically at stationary PGE electrodes, as well as at stationary carbon felt.[33] Carbon felt is a low-cost, high surface area web of amorphous carbon fibers.[41] Large numbers of hydrogenase can potentially adsorb to the high internal surface area of this material. This feature makes the carbon felt electrode amenable to device applications, where cell geometry may constrain the electrode size. Although the *Ca*HydA signal at stationary electrodes can be complicated by mass transport, it is relevant to the performance of these electrodes in the photoelectrochemical biofuel cell.

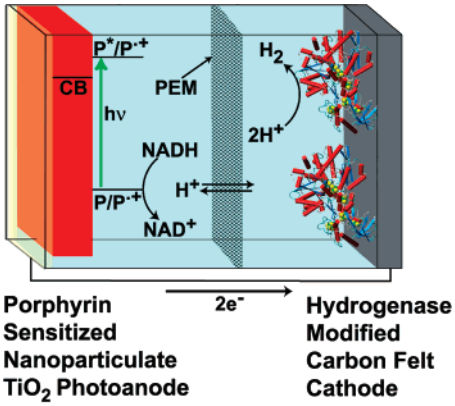

Figure 1. Schematic drawing of the photoelectrochemical cell used in this work.

The carbon felt/*Ca*HydA electrode was tested as the cathode in this photoelectrochemical biofuel cell (Figure 1) and compared to the cell operating with a platinum cathode.[42] The cell uses a dye-sensitized nanoparticulate TiO_2 photoanode, supported on a transparent, conductive fluorine-doped tin(IV) oxide (FTO) substrate.[43,44] The photoanode serves to generate a charge separated state, reminiscent of molecular reaction centers.[45] Photon absorption, by the sensitizer porphyrin (P), leads to a porphyrin excited singlet state (P*), which relaxes via electron transfer to the TiO_2 conduction band (CB). This process occurs in parallel at multiple sites along the porphyrin−TiO_2 interface. The resulting radical cations ($P^{\bullet+}$), residing on surface-bound dye molecules, oxidize NADH through two stepwise, one-electron processes, regenerating ground-state porphyrins for further rounds of light excitation. The accumulation of NAD^+ in the anode solution is able to drive the NAD-linked enzymatic oxidation of an appropriate biofuel substrate.[46] The injected

(27) Jones, A. K.; Sillery, E.; Albracht, S. P. J.; Armstrong, F. A. *Chem. Commun.* **2002**, 866−867.
(28) Frey, M. *ChemBioChem* **2002**, *3*, 153−160.
(29) Buhrke, T.; Lenz, O.; Krauss, N.; Friedrich, B. *J. Biol. Chem.* **2005**, *280*, 23791−23796.
(30) Yaropolov, A. I.; Karyakin, A. A.; Varfolomeev, S. D.; Berezin, I. V. *Bioelectrochem. Bioenerg.* **1984**, *12*, 267−277.
(31) Bianco, P.; Haladjian, J. *J. Electrochem. Soc.* **1992**, *139*, 2428−2432.
(32) Karyakin, A. A.; Morozov, S. V.; Karyakina, E. E.; Varfolomeyev, S. D.; Zorin, N. A.; Cosnier, S. *Electrochem. Commun.* **2002**, *4*, 417−420.
(33) Morozov, S. V.; Vignais, P. M.; Cournac, L.; Zorin, N. A.; Karyakina, E. E.; Karyakin, A. A.; Cosnier, S. *Int. J. Hydrogen Energy* **2002**, *27*, 1501−1505.
(34) Johnston, W.; Cooney, M. J.; Liaw, B. Y.; Sapra, R.; Adams, M. W. W. *Enzyme Microb. Technol.* **2005**, *36*, 540−549.
(35) Lamle, S. E.; Vincent, K. A.; Halliwell, L. M.; Albracht, S. P. J.; Armstrong, F. A. *Dalton Trans.* **2003**, 4152−4157.
(36) Rüdiger, O.; Abad, J. M.; Hatchikian, E. C.; Fernandez, V. M.; De Lacey, A. L. *J. Am. Chem. Soc.* **2005**, *127*, 16008−16009.
(37) King, P. W.; Posewitz, M. C.; Ghirardi, M. L.; Seibert, M. *J. Bacteriol.* **2006**, *188*, 2163−2172.
(38) Peters, J. W.; Lanzilotta, W. N.; Lemon, B. J.; Seefeldt, L. C. *Science* **1998**, *282*, 1853−1858.
(39) Adams, M. W. W.; Mortenson, L. E. *J. Biol. Chem.* **1984**, *259*, 7045−7055.
(40) Adams, M. W. W. *Biochim. Biophys. Acta* **1990**, *1020*, 115−145.
(41) Ateya, B. G.; Al-Kharafi, F. M.; Abdallah, R. M.; Al-Azab, A. S. *J. Appl. Electrochem.* **2005**, *35*, 297−303.
(42) Hambourger, M.; Brune, A.; Gust, D.; Moore, A. L.; Moore, T. A. *Photochem. Photobiol.* **2005**, *81*, 1015−1020.
(43) Grätzel, M. *Inorg. Chem.* **2005**, *44*, 6841−6851.
(44) Brune, A.; Jeong, G.; Liddell, P. A.; Sotomura, T.; Moore, T. A.; Moore, A. L.; Gust, D. *Langmuir* **2004**, *20*, 8366−8371.
(45) Durrant, J. E.; Haque, S. A.; Palomares, E. *Chem. Commun.* **2006**, 3279−3289.
(46) de la Garza, L.; Jeong, G.; Liddell, P. A.; Sotomura, T.; Moore, T. A.; Moore, A. L.; Gust, D. *J. Phys. Chem. B* **2003**, *107*, 10252−10260.

electrons, residing in the TiO_2 conduction band, provide reducing equivalents to the cathode, where hydrogen production occurs.[42,47] Small cations exchange across the proton exchange membrane (PEM) to balance charge. Productive electron transfers are in competition with nonproductive recombination reactions occurring between TiO_2 conduction band electrons and oxidized species at the photoanode surface. The potential of the cathode influences the electron density in the TiO_2 conduction band and, hence, the rate of recombination.[48] The overall function of this device is to photochemically reform biomass to H_2. The photochemical step overcomes the activation energy for the one-electron oxidation of NADH and often stores a portion of the incident photon energy in the H_2 product, depending upon the type of biomass used.

Experimental Section

[FeFe]-hydrogenase *Ca*HydA from *C. acetobutylicum* was expressed in *Escherichia coli*, purified, and assayed for H_2 evolution and H_2 uptake activities according to previously reported procedures.[37,39] As is typical for [FeFe]-hydrogenases, *Ca*HydA is irreversibly inhibited upon exposure to O_2, with a half-life of only a few minutes in air.[49] For this reason, enzyme isolation and all experiments were conducted in a glovebox under strictly anaerobic conditions (2−3% H_2, bulk N_2, <1 ppm O_2). Under these conditions (and at ambient temperature, ~30 °C), *Ca*HydA was quite stable and degradation was not observed during short-term (≤5 h) testing in the photoelectrochemical cell. *Ca*HydA activity units (U) were defined as 1 μmol H_2 produced or consumed per minute. The work presented was performed with three separate preparations of *Ca*HydA, with nominal specific activities (for H_2 production) of 130, 290, and 400 U mg^{-1}.

Cyclic voltammetry was performed with a CH Instruments 650C electrochemical workstation using a platinum foil counter electrode and a Ag/AgCl (saturated KCl) reference electrode. A vycor frit, separating the counter and working solutions, was used as needed to minimize *Ca*HydA inhibition due to O_2 generation at the counter electrode. All values in this article are referenced versus Ag/AgCl (saturated KCl). Potentials on the Ag/AgCl reference scale can be converted to the standard hydrogen electrode reference scale by adding 0.199 V to the value reported vs Ag/AgCl.

Pyrolytic graphite edge, glassy carbon, carbon felt, and platinum electrodes were cleaned before use, by either polishing or heat treatment. The electrochemically active surface area for each type of electrode was determined from cyclic voltammograms of ferricyanide. *Ca*HydA was adsorbed to the stationary electrode while repeatedly cycling the voltage in a dilute hydrogenase solution (1.6 U mL^{-1}) until a stable signal was obtained. The adsorbed hydrogenase films were rinsed with deionized water and transferred to fresh buffer solutions for characterization. Coadsorbates, such as polymyxin B sulfate, were not used in the present study. All cyclic voltammograms were initiated at the most positive potential. In each plot, arrows indicate the direction of the scan. Current densities were determined in terms of the electrochemically active surface area.

TiO_2 electrodes were prepared according to a literature procedure[50] and sensitized with 5-(4-carboxyphenyl)-10,15,20-tris(4-methylphenyl)-porphyrin.[51] The two-compartment photoelectrochemical cell was assembled as previously described.[47] Carbon felt or platinum foil of comparable electrochemically active surface area (~3.5 cm^2) served as the cathode. Illumination was provided by either a light-emitting diode (λ_{max} = 520 nm, peak width at half-height = 50 nm, 3 mW cm^{-2}) or a filtered Hg arc lamp (λ = 550 ± 10 nm, ~50 mW cm^{-2}). The anode and cathode solutions consisted of 0.1 M sodium phosphate buffer (pH 7.0), with 10 mM NADH added to the anode solution. For hydrogenase cathodes, an adsorbed *Ca*HydA film was formed on carbon felt before testing in the photoelectrochemical cell. Except where indicated otherwise, excess *Ca*HydA was maintained in the cathodic solution to minimize enzyme desorption. Photocurrent was determined as the short circuit current under illumination minus the short circuit current in the dark. Hydrogen production was determined by gas chromatography. A more detailed description of the materials and methods used in this work is available in the Supporting Information.

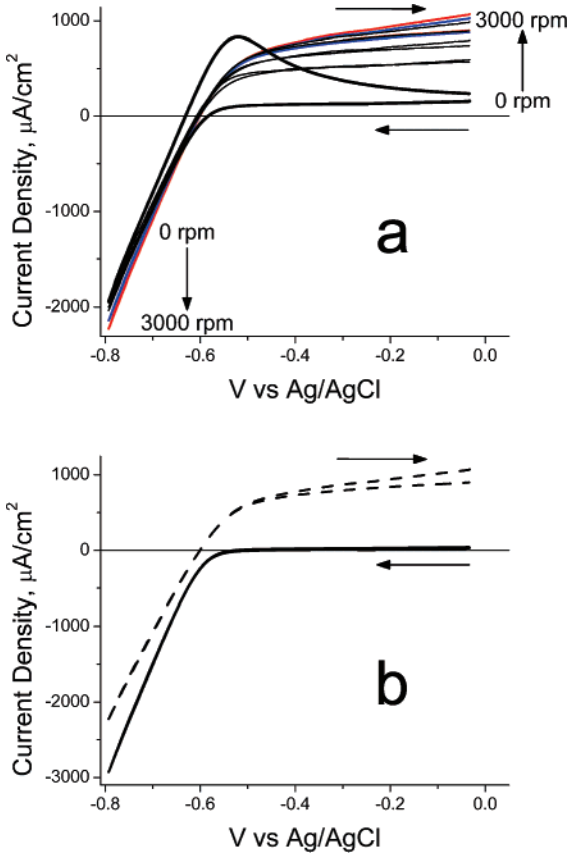

Figure 2. Cyclic voltammograms of a *Ca*HydA film adsorbed to a PGE electrode in (a) H_2-saturated buffer at various rotation rates [0 (thick black line), 200, 500, 1000, 2000 (blue line), 3000 (red line) rpm] or (b) H_2 (− − −) or Ar (—) saturated buffer at 3000 rpm. Conditions are 0.1 M phosphate, pH 7.0, ν = 50 mV s^{-1}.

Results and Discussion

Cyclic Voltammetry of *Ca*HydA. When placed in a dilute hydrogenase solution, both PGE and carbon felt electrodes exhibited increasing current with repetitive voltage scans, consistent with the adsorption of hydrogenase at the electrode surface (Supporting Information Figure S1). When these electrodes were rinsed with deionized water and transferred to a fresh buffer solution, the electrochemical signal was retained, indicating an adsorbed hydrogenase layer. Figure 2a shows the effect of electrode rotation for an adsorbed PGE/*Ca*HydA electrode in H_2-saturated, pH 7.0, buffer. At all rotation rates the waveform reflects the catalytic activity of *Ca*HydA and is characteristic of proton reduction at cathodic (i.e., more negative) potentials and hydrogen oxidation at anodic (i.e., more positive)

(47) Hambourger, M.; Liddell, P. A.; Gust, D.; Moore, A. L.; Moore, T. A. *Photochem. Photobiol. Sci.* **2007**, *6*, 431−437.
(48) Haque, S. A.; Tachibana, Y.; Willis, R. L.; Moser, J. E.; Grätzel, M.; Klug, D. R.; Durrant, J. R. *J. Phys. Chem. B* **2000**, *104*, 538−547.
(49) Ghirardi, M. L.; Posewitz, M. C.; Maness, P.-C.; Dubini, A.; Yu, J.; Seibert, M. *Annu. Rev. Plant Biol.* **2007**, *58*, 71−91.
(50) Kang, M. G.; Park, N.-G.; Park, Y. J.; Ryu, K. S.; Chang, S. H. *Sol. Energy Mater. Sol. Cells* **2003**, *75*, 475−479.
(51) Anton, J. A.; Kwong, J.; Loach, P. A. *J. Heterocycl. Chem.* **1976**, *13*, 717−725.

potentials.[16] In the initial scan toward more negative potentials, a plateau of positive (anodic) current, attributed to hydrogen oxidation, gives way to a sloping region of negative (cathodic) current, corresponding to proton reduction. The transition between hydrogen oxidation and proton reduction occurs at the point of zero current, which equates to the formal potential of the H^+/H_2 couple under the experimental conditions.[21] This value is dependent upon the local concentrations of H^+ and H_2 at the electrode surface, which are influenced by the catalytic activity of *Ca*HydA, the rate of working electrode rotation, and the concentrations in the bulk solution.

The catalytic turnover of *Ca*HydA is sufficiently fast that, for the stationary electrode (Figure 2a), the mass transport of H_2 strongly influences the electrochemical signal.[15,21] On the forward scan, H_2 depletion at the electrode surface results in low anodic currents and shifts the point of zero current to a more positive potential. In the cathodic region, proton reduction increases the surface concentration of H_2. The accumulated H_2 shifts the point of zero current negative on the reverse scan. The reverse scan also shows a distinctive anodic peak due to the oxidation of surface accumulated H_2.[16,23] The position of this peak varies with the scan rate and cathodic range, reflecting the relative time scales of the experiment and the diffusion of H_2 away from the electrode (Supporting Information Figure S2). The persistence of this peak in a hydrogen "saturated" solution indicates a high local concentration of H_2 at the electrode surface (i.e., the observed formation of H_2 bubbles) and a substantial reductive catalytic ability of *Ca*HydA.

With sufficiently fast rotation of the working electrode (~2000 rpm in Figure 2a), the surface concentrations of H^+ and H_2 approach those in the bulk solution and are essentially constant. Under these conditions, mass transport no longer governs the catalytic signal. As a result, there is a loss of the hydrogen oxidation peak, a significant increase in the hydrogen oxidation plateau current, a smaller increase in the cathodic current, and the forward and reverse scans become virtually superimposable. Under these conditions, the point of zero current (−0.602 V) reflects the concentrations of H^+ and H_2 in the bulk solution and is quite close to the expected Nernstian value (−0.613 V) for the H^+/H_2 couple at pH 7.0 under 1 atm of H_2. The slight deviance may indicate incomplete hydrogen saturation of the bulk solution in the open-topped electrochemical cell used with the rotating disc electrode.

Close to the point of zero current, interfacial electron transfer is slow and the rate of reduction or oxidation of the enzyme limits the catalytic turnover.[16] As the applied voltage is shifted in either direction away from this value, the driving force for and hence the rate of interfacial electron transfer increases. As a result, increasing currents are observed until interfacial electron transfer becomes fast relative to enzymatic turnover. With this condition satisfied, the current is independent of the applied bias and a limiting current plateau is expected in the voltammograms, with the limiting current proportional to the inherent turnover rate of the enzyme in the presence of the experimental surface concentrations of substrate and product.[35] In Figure 2a, the presence of an anodic limiting current indicates that, in this region, the rate of enzymatic H_2 oxidation is slow relative to the rate of interfacial electron transfer. The absence of a cathodic limiting current then suggests a relatively higher turnover number for proton reduction. Supporting Information Figure S3 shows that a cathodic limiting current is not reached when scanning as negative as −1.2 V. Assuming the rates of interfacial electron transfer are similar in both directions (i.e., there is no major reorientation of the adsorbed enzyme film as a function of potential), then the absence of a cathodic limiting current indicates a catalytic bias of *Ca*HydA toward proton reduction under the conditions studied.

Further information supports this proposed catalytic bias. At fast rotation rates, the ratio of cathodic and anodic currents reflects the catalytic bias of *Ca*HydA under the substrate conditions of the bulk solution. In Figure 2a, at 3000 rpm in H_2-saturated solution, the ratio of cathodic divided by anodic current densities ranges from 1.1 at low overpotentials (i.e., close to the point of zero current) to 2.9 at 192 mV overpotential (Supporting Information Figure S4). At all overpotentials investigated, the current densities were greater for proton reduction even though the concentration of protons (10^{-7} M) is nearly 4 orders of magnitude less than the concentration of hydrogen ($\sim 8 \times 10^{-4}$ M).[52] Additionally, Figure 2b shows voltammograms obtained for a *Ca*HydA film at high rotation rates in either argon- or hydrogen-saturated pH 7.0 buffer. Supporting Information Figure S5 shows a series of rotation rates in argon-saturated buffer. In the absence of H_2, there is essentially no anodic current, and the point of zero current is shifted positive. In the presence of H_2, there is a notable increase in the hydrogen oxidation current, and there is only a modest inhibition of proton reduction. In contrast, the proton reduction activity of [NiFe]-hydrogenases, with a catalytic bias toward H_2 oxidation, is substantially inhibited under 1 atm H_2.[15,21] The strong cathodic signal for the [FeFe]-hydrogenase *Ca*HydA, even under 1 atm H_2, attests to the impressive catalytic activity of this enzyme in the hydrogen evolution reaction.

This finding stands in contrast to a previous report of solution-based biochemical assays of *Ca*HydA, which shows a catalytic bias toward H_2 oxidation. In that study, the rate of H_2 oxidation was, surprisingly, found to be 1000 times greater than that of H^+ reduction.[53] In our hands, similar solution-based assays using oxidized and reduced methyl viologen showed a more modest bias toward H_2 oxidation, with specific activities of 253 ± 47 and 80 ± 7 U mg^{-1} in the H_2 uptake and H_2 production reactions, respectively. This yields a ratio of ~3:1 in favor of H_2 oxidation, similar to literature values for the closely related CpI [FeFe]-hydrogenase.[39] The cause for the discrepancy between the electrochemical and solution-based assays is not fully resolved at present. However, it is not surprising to find differences when using either the electrode or a soluble electron mediator as the redox partner for *Ca*HydA in disparate assay procedures.

It should be noted that the voltammograms in Figure 2 also indicate a heterogeneous surface, with a distribution of hydrogenase orientations. As the driving force for interfacial electron transfer increases, new populations of hydrogenase in suboptimal orientations become catalytically active.[16,17] This heterogeneity is the presumed source of the residual slope in the anodic limiting current plateau and likely contributes to the lack of an observable cathodic limiting current. Heterogeneity also implies that improved electrode performance is likely to be obtained

(52) Crozier, T. E.; Yamamoto, S. *J. Chem. Eng. Data* **1974**, *19*, 242−244.
(53) Girbal, L.; von Abendroth, G.; Winkler, M.; Benton, P. M. C.; Meynial-Salles, I.; Croux, C.; Peters, J. W.; Happe, T.; Soucaille, P. *Appl. Environ. Microbiol.* **2005**, *71*, 2777−2781.

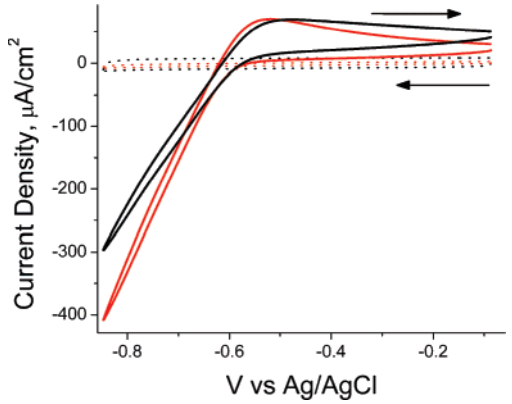

Figure 3. Comparison of stationary pyrolytic graphite edge (red lines) and carbon felt (black lines) electrodes, before (···) and after (—) adsorption of *Ca*HydA. Conditions are 0.1 M phosphate, pH 7.0, $\nu = 10$ mV s^{-1}, 2−3% H_2, bulk N_2 atmosphere.

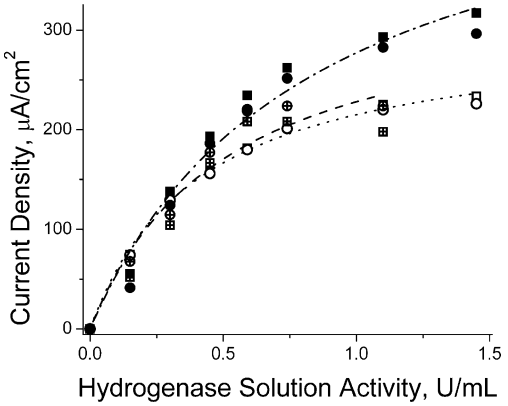

Figure 4. Cathodic current densities (determined at −0.85 V) as a function of *Ca*HydA activity in solution for PGE (closed symbols), carbon felt (open symbols), and glassy carbon (cross-hatched symbols) electrodes; for scans at 50 mV s^{-1} (squares) and 10 mV s^{-1} (circles). Data were fit to Langmuir adsorption isotherms for PGE (· − ·), carbon felt (···), and glassy carbon (− − −) electrodes. Conditions are 0.1 M phosphate, pH 7.0, 2−3% H_2, bulk N_2 atmosphere, $\omega = 0$ rpm.

through better control of the hydrogenase orientation, which should enhance electronic communication as compared to the enzyme adsorbed to the electrode surface in random orientations.[36]

The data obtained at the rotating disc PGE electrode indicate that *Ca*HydA is an active catalyst for proton reduction, amenable to direct electron transfers with a carbon electrode. Integration of this catalyst into the photoelectrochemical biofuel cell is most readily achieved at a stationary cathode. For this purpose, immobilized *Ca*HydA was studied electrochemically at stationary PGE and carbon felt electrodes. These materials have different surface morphologies, which may favor or disfavor specific interactions with *Ca*HydA. The PGE electrode has a large surface area due to pores and trenches penetrating between graphite sheets, although much of this area may be inaccessible to *Ca*HydA or part of the poorly conductive graphite basal plane.[54] Carbon felt is a porous three-dimensional material with a high internal surface area.[41] Under the conditions studied, both types of carbon are expected to have primarily acidic, oxygen-containing functional groups at "dangling bond" defect sites on the electrode surface.[55,56] The specific surface chemistry of each electrode was not examined in this work.

Figure 3 shows cyclic voltammograms of hydrogenase films adsorbed to stationary PGE and carbon felt electrodes. The current densities are lower than those in Figure 2, a result of this work being performed with a preparation of *Ca*HydA having a lower specific activity. Aside from the amplitude of the electrochemical signal, the waveform is broadly consistent with that in Figure 2 and subject to the same interpretations. Both types of carbon exhibit similar behavior with *Ca*HydA and relatively similar current densities (determined by the electrochemically active surface area). The most notable differences between the two materials are the modestly higher initial anodic current densities, the lower cathodic current densities, and the broader hydrogen reoxidation peak observed at carbon felt. These variations can be explained by differential rates of H_2 diffusion away from the PGE and carbon felt surfaces. The three-dimensional structure of carbon felt readily entraps H_2 bubbles during the cathodic sweep, slowing the rate of H_2 diffusion away from the electrode. For carbon felt, the retention of H_2 produced during previous cycles gives rise to the higher initial anodic currents and a slight negative shift in the point of zero current during the forward scan. On the reverse scan, the retention of H_2 at the carbon felt electrode results in a broadening of the hydrogen reoxidation signal, since the surface concentration of H_2 is changing more slowly relative to the time scale of the measurement. The retention of hydrogen in pores of the carbon felt may also lead to H_2 inhibition of the cathodic current, as demonstrated for *Ca*HydA in Figure 2b. The cathodic current densities, in Figure 3, could also reflect differences in the surface density and orientation of adsorbed active *Ca*HydA on the two types of carbon. For a stationary carbon felt/*Ca*HydA electrode, the assignment of the cathodic wave as H_2 production was confirmed by poising the electrode at −0.94 V for 60 min, followed by determination of the headspace composition by gas chromatography. During electrolysis, 15.6 μmol of electrons were passed through the circuit and 8.46 ± 0.85 μmol of H_2 were produced, giving a Faradaic efficiency of 1.08 ± 0.11 for H_2 production (Supporting Information Figure S6).

Figure 4 shows the cathodic current densities for stationary electrodes with *Ca*HydA adsorbed from solutions of different enzyme concentration. For each point, the electrode was placed into solution and the potential was cycled until a stable current response was achieved. The effect was studied at both PGE and carbon felt electrodes, as well as at glassy carbon electrodes, which gave generally comparable voltammograms for adsorbed *Ca*HydA (Supporting Information Figure S2a). For all three types of carbon electrodes, the cathodic current density increased with increasing concentrations of hydrogenase in solution, until a plateau region was approached at sufficiently high concentrations. This concentration dependence of the catalytic current indicates an equilibrium between unbound and bound *Ca*HydA, with a larger concentration of bound enzyme as the concentration of unbound enzyme is increased. All three series were fit to Langmuir adsorption isotherms, indicating that catalytic current is proportional to the fractional surface coverage of active, oriented hydrogenase.

Electrochemical H_2 Evolution Compared at *Ca*HydA and Platinum Electrodes. Interest in hydrogenase electrodes stems

(54) Blanford, C. F.; Armstrong, F. A. *J. Solid State Electrochem.* **2006**, *10*, 826−832.
(55) Boehm, H. P. Carbon Surface Chemistry. In *Graphite and Precursors;* Delhaès, P., Ed.; World of Carbon; Gordon & Breach: Australia, 2001; pp 141−178.
(56) Bond, A. M. *Anal. Proc.* **1992**, *29*, 132−148.

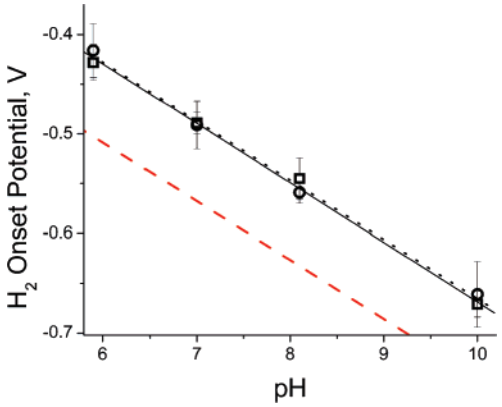

Figure 5. pH dependence of the onset of hydrogen evolution at stationary PGE/*Ca*HydA (○) and platinum (□) electrodes. For the *Ca*HydA series, enzyme adsorption was performed at pH 7.0 and the electrode was equilibrated at the indicated pH before measurement. Linear regression lines are plotted for the PGE/*Ca*HydA ($y = -0.0594x - 0.0711$; •••) and platinum ($y = -0.0598x - 0.0704$; —) electrodes. The red dashed line indicates the potential of the H^+/H_2 couple at pH 7.0 and 0.03 atm H_2. Conditions are 0.1 M phosphate, $\nu = 50$ mV s^{-1}, 2−3% H_2, bulk N_2 atmosphere.

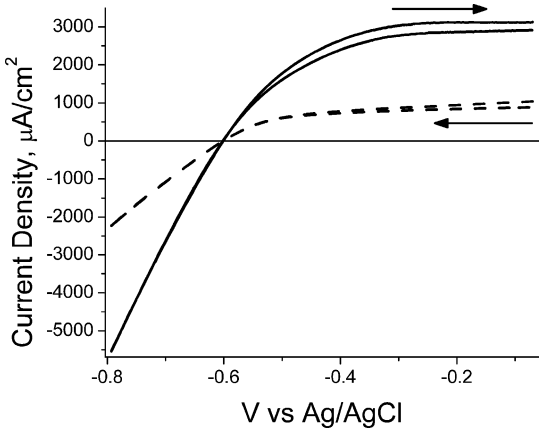

Figure 6. Comparison of platinum (—) and *Ca*HydA modified PGE (− − −) rotating disc electrodes, both in H_2-saturated buffer. Conditions are 0.1 M phosphate, pH 7.0, $\nu = 50$ mV s^{-1}, $\omega = 3000$ rpm.

in part from the possibility that enzymatic catalysts may replace platinum in hydrogen fuel cells and hydrogen production systems. Jones et al. have previously compared the catalytic ability of [NiFe]-hydrogenase electrodes directly to platinum in the hydrogen oxidation reaction.[27] They demonstrated that at low H_2 partial pressures the performance of these two catalysts is nearly identical, whereas under 1 atm H_2 [NiFe]-hydrogenase can still give anodic current densities similar to that of platinum, although at higher overpotentials. To the best of our knowledge, the same comparison has not been made for the hydrogen evolution reaction. As described above, the [FeFe]-hydrogenase *Ca*HydA has a catalytic bias toward hydrogen production and exhibits high cathodic current densities when immobilized on a variety of carbon electrodes. Thus, *Ca*HydA is an interesting catalyst for comparison to platinum. Two aspects of the catalytic signal were examined: the potential at which catalysis begins and the current densities obtained at a given overpotential.

As shown in Figure 5, both platinum and PGE/*Ca*HydA electrodes are effective catalysts operating near the reversible potential of the H^+/H_2 redox couple. At the low partial pressures of H_2 used, the point of zero current is poorly defined. Instead, we report on the onset of hydrogen production, estimated from the first derivative of the cyclic voltammograms. Over the pH range 6−10, for both platinum and hydrogenase electrodes, the onset of H_2 production occurs ∼80 mV positive of the Nernstian H^+/H_2 potential of the bulk solution (red dashed line in Figure 5). This offset is attributed to the depletion of H_2 at the stationary electrode surface during the anodic portion of the forward scan. Attempts to study *Ca*HydA under more acidic conditions were unsuccessful. At pH 5.1, the onset potential was the same as that at pH 5.9, suggesting that the residual catalytic signal was due to *Ca*HydA that had not yet equilibrated with the pH 5.1 solution. At this low pH, the catalytic current decreased with increased exposure time to the buffer and a stable current response could not be obtained. However, in our laboratory, solution-based methyl viologen assays[39] showed that *Ca*HydA remained active at pH 5.1. These two results likely indicate that desorption of the enzyme from the electrode, at pH 5.1, leads to the loss of the catalytic signal. For the same pH series, the current densities 120 mV negative of the onset potential indicate an optimal catalytic activity near neutral pH (Supporting Information Figure S7).

Figure 6 shows the electrochemical response of a PGE/*Ca*HydA electrode compared directly to that of platinum. In both cases, cyclic voltammograms were recorded in H_2-saturated phosphate buffer (pH 7.0) at high rotation rates. The hydrogenase data set is the same as presented in Figure 2b. Additional voltammograms for the platinum rotating disc electrode are shown in Supporting Information Figure S8. In general, the shape of the catalytic wave is quite similar for both the *Ca*HydA and platinum electrodes. The anodic limiting current plateau at high rotation rates suggests that the low solubility of H_2 in the bulk solution limits the rate of H_2 oxidation for both catalysts. The point of zero current varies by less than 2 mV between the two traces, consistent with the results in Figure 5. Comparison of the current densities indicates that the platinum surface is the more active catalyst, although the randomly oriented *Ca*HydA electrode is only a factor of 2 or 3 worse. In the cathodic region, the hydrogenase current densities are ∼40% of those obtained at platinum. In the anodic plateau, this ratio ranges from 29 to 35% depending upon the potential. The performance, relative to that of platinum, of *Ca*HydA in the anodic and cathodic regions is yet another line of evidence suggesting that *Ca*HydA has a catalytic bias toward proton reduction. The lower current densities obtained with *Ca*HydA, as compared to that of platinum, can be attributed to the lower surface coverage of active catalytic sites. Given that the theoretical maximum surface density of immobilized *Ca*HydA [FeFe]-hydrogenase (∼3.3 pmol cm^{-2}, based on an estimated 50 nm^2 footprint for each molecule)[38] is considerably less than the surface density of catalytic sites on the platinum surface (∼1.1 nmol cm^{-2}),[57] it seems likely that *Ca*HydA is more active per catalytic site.[27] It is worth pointing out that in this study the enzyme adsorption process has not been optimized, and higher current density for *Ca*HydA electrodes may likely be obtained. In the absence of a noncatalytic electrochemical signal for *Ca*HydA, we are presently unable to precisely quantify the surface coverage of electroactive hydrogenase or report a valid turnover number for this enzyme on the electrode surface.

Photoelectrochemical Hydrogen Production Catalyzed by *Ca*HydA. One application of hydrogenase electrodes is their

(57) Watson, G. W.; Wells, R. P. K.; Willock, D. J.; Hutchings, G. J. *Chem. Commun.* **2000**, 705−706.

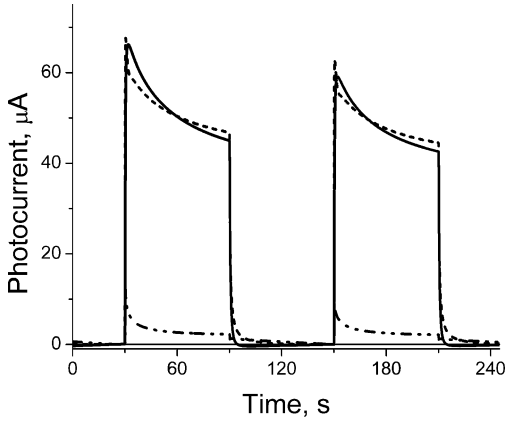

Figure 7. Short circuit photocurrent of the photoelectrochemical cell with either a carbon felt (· · −), carbon felt/*Ca*HydA (—), or platinum foil (− − −) cathode. In each case, the electrochemically active surface area of the cathode was ∼3.5 cm^2. (520-nm illumination, 3 mW cm^{-2}).

use in photochemical energy conversion systems. In view of the challenge of extracting electrosynthetic work from such systems, and to further compare hydrogen production on platinum to that catalyzed by *Ca*HydA, the carbon felt/*Ca*HydA electrodes were tested as the cathode in a photoelectrochemical biofuel cell. In these experiments, NADH was used as a sacrificial electron donor. The ability of this system to recycle NAD^+ and use a biological substrate as an electron source has been previously established.[42,46] In the photoelectrochemical cell, the cathodic potential is determined by the surface concentrations of H^+ and H_2. In the light, photochemical charge separation shifts the TiO_2 quasi-Fermi level negative of this value, generating photovoltage and photocurrent.[43] The offset between these two values, and the occupancy of conduction band/trap states in the TiO_2, influences the net efficiency of the (photo)-chemical reactions at the photoanode, which include electron recombination.[48]

Figure 7 shows the cell short circuit photocurrent during 1-min light and dark cycles. The current decay occurring during illumination is likely related to the accumulation of hydrogen at the cathode surface, as well as the local depletion of NADH near the photoanode.[58] In the absence of hydrogenase, the carbon felt cathode resulted in negligible photocurrents. In the presence of *Ca*HydA, the carbon felt cathode gave photocurrents comparable to a platinum electrode. Supporting Information Figure S9 shows that starting with a clean, unmodified carbon felt cathode the short circuit photocurrent increased with increasing quantities of *Ca*HydA added to the cathode solution, similar to the electrochemical results shown in Figure 4. In experiments under higher light intensity, the hydrogen product in the cathode headspace was quantified by gas chromatography. No hydrogen product was detected for the carbon felt cathode without *Ca*HydA present. The average rates of hydrogen production over an ∼60-min illumination period (23.4 nmol H_2 min^{-1} for carbon felt/*Ca*HydA versus 19.8 nmol H_2 min^{-1} for platinum) were nearly identical whether using a platinum or hydrogenase cathode (Supporting Information Figure S10). With known quantities of *Ca*HydA immobilized on the carbon felt cathode, and no excess *Ca*HydA in the cathode solution, the rate of hydrogen production (averaged over ∼20 min of

(58) Vlachopoulos, N.; Liska, P.; McEvoy, A. J.; Grätzel, M. *Surf. Sci.* **1987**, *189/190*, 823−831.

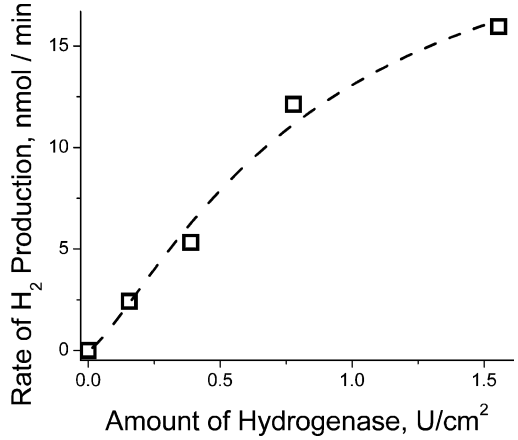

Figure 8. Rate of H_2 production in the photoelectrochemical cell (determined by gas chromatography) as a function of the quantity of *Ca*HydA immobilized on the carbon felt cathode. Known quantities of *Ca*HydA solution were pipetted onto carbon felt and allowed to soak into the material and dry. Units of *Ca*HydA deposited per electrochemically active area (∼3.5 cm^2) are shown in the figure. For these data, no excess *Ca*HydA was present in solution. 550-nm illumination, ∼50 mW cm^{-2}.

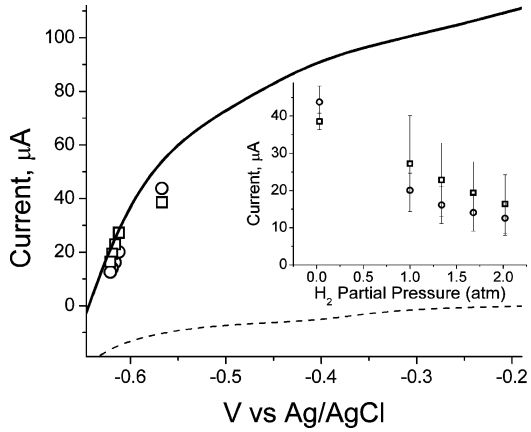

Figure 9. Current−voltage profile of the photoanode (ν = 5 mV s^{-1}) run in a three-electrode configuration under 520-nm (3 mW cm^{-2}) illumination (—) and in the dark (− − −). Superimposed on the *I*−*V* profile is the short circuit current for the cell in a two-electrode configuration (520-nm illumination, 3 mW cm^{-2}), with increasing pressures of H_2 above the cathode solution, using a carbon felt/*Ca*HydA (□) or platinum (○) cathode. The inset shows the raw hydrogen back pressure data before being converted to V vs Ag/AgCl by application of the Nernst equation: $E_{H^+/H_2} = E° - 0.0296*\log(P_{H_2}) - 0.0591*pH$.

illumination) is shown to depend upon the quantity of immobilized *Ca*HydA (Figure 8). Supporting Information Figure S11 shows the H_2 production kinetic traces from which Figure 8 was created. It should be noted that within the photoelectrochemical cell *Ca*HydA remains extremely oxygen sensitive, and opening the cell to air leads to the rapid loss of hydrogenase activity.

Figure 9 shows a current−voltage profile of the photoanode in a three-electrode configuration. In this configuration, the photoanode is isolated by the potentiostat circuit, and performance is independent of the cathode. The bias applied by the potentiostat controls the Fermi level of the FTO substrate of the photoanode. The electron density in the TiO_2 conduction band increases as the applied bias is swept to more negative potentials. Since charge recombination can occur from any conduction band electron, or from exposed regions of the FTO substrate, as the electron density increases so does the probability of recombination.[48] In the photoelectrochemical cell described

in this work, electron recombination to NAD^+ in solution is thermodynamically disfavored, and charge recombination to oxidized sensitizer dyes is the dominant loss mechanism.[47] This process limits the short circuit current under illumination as recombination becomes competitive with the regeneration of ground-state sensitizer dyes by NADH in solution.[59] This effect gives rise to the shape of the $I-V$ profile in Figure 9. The voltage at which the current (of the illuminated device) goes to zero is an approximation of the quasi-Fermi level of the TiO_2 under illumination. This point sets a cathodic limit for the potential at which work can be extracted from the photoelectrochemical cell, under the illumination regime tested.

When the photoanode is directly wired to a cathode, in a two-electrode configuration, the cathode determines the Fermi level of the FTO substrate of the photoanode, in a manner analogous to a bias applied by a potentiostat. The inset of Figure 9 shows the short circuit current (under 520-nm illumination) as the H_2 pressure above the cathode solution is increased. Both platinum and *Ca*HydA electrodes exhibited a similar decrease in current upon increasing the hydrogen pressure in the cathode headspace. This effect can be rationalized in terms of the increasing pressures of hydrogen shifting the cathode to more negative potentials, thereby increasing the rate of charge recombination and decreasing the current of the device. The partial pressures of hydrogen, shown in the inset, were converted to V vs Ag/AgCl according to the Nernst equation. The resulting data points are superimposed on the $I-V$ curve shown in Figure 9. There is good agreement between the two experimental methods, with comparable currents at a given potential, whether that potential is applied with a potentiostat or with H_2 back pressure.

The hydrogen back pressure data points at -0.57 V are the short circuit current of the photoelectrochemical cell run in a two-electrode configuration under low partial pressures of hydrogen (0.03 atm). The portion of the current−voltage curve to the left of this point is essentially the $I-V$ profile of the photoelectrochemical cell when the anode is directly wired to the cathode. This portion of the $I-V$ curve exhibits ohmic behavior, indicating that there is insufficient driving force to maintain the diode effect of the illuminated device. This situation depends in part on the intensity of the light incident upon the photoanode.[60] However, the output voltage of the photoanode is largely constrained by the density of states near the conduction band edge, which is a function of the semiconductor material and the electrolyte conditions.[48] The data presented suggest that the conduction band edge of the TiO_2 semiconductor used in this work is not sufficiently reducing for high rates of hydrogen production. Since both *Ca*HydA and platinum electrodes operate near the reversible H^+/H_2 potential, they have a similar influence on the TiO_2 conduction band electron density and, hence, the rate of recombination. As a result, with sufficient hydrogenase present, the platinum and *Ca*HydA cathodes performed comparably in the photochemical experiments, and the photoanode was the limiting factor in both cases.

(59) Cahen, D.; Hodes, G.; Grätzel, M.; Guillemoles, J. F.; Riess, I. *J. Phys. Chem. B* **2000**, *104*, 2053−2059.
(60) Liu, Y.; Hagfeldt, A.; Xiao, X.-R.; Lindquist, S.-E. *Sol. Energy Mater. Sol. Cells* **1998**, *55*, 267−281.

Conclusions

In summary, *C. acetobutylicum* [FeFe]-hydrogenase HydA (*Ca*HydA) was immobilized at carbon electrodes, characterized electrochemically, and tested for hydrogen production in a photoelectrochemical biofuel cell. The electrochemical response of the *Ca*HydA electrodes was broadly similar among the types of carbon tested and generally consistent with literature reports of [FeFe]-hydrogenase electrochemistry.[23−25] Under these experimental conditions, the *Ca*HydA hydrogenase exhibits a catalytic bias toward hydrogen production, in contrast with a previous report.[53] In cyclic voltammograms, *Ca*HydA electrodes showed cathodic current densities ∼40% of those obtained at a platinum electrode. Given the disparate surface densities of hydrogenase and platinum catalytic centers, it is likely that the turnover frequency of individual catalytic sites is greater for *Ca*HydA than that for platinum. Improved packing and orientation of active hydrogenase at the electrode surface, for example by reducing the enzyme "footprint" through structural minimization,[37] could potentially produce a hydrogen electrode that is superior to platinum.

One of the electrodes tested was a high surface area carbon felt. This low-cost material allows a large number of hydrogenase enzymes to be electrically contacted at a compact electrode. As a result, the carbon felt electrode exhibits a cathodic current density considerably higher than platinum foil in terms of the nominal two-dimensional area, due to the high internal surface area. This feature makes carbon felt an interesting material for device applications, where two-dimensional area can be a relevant parameter. These carbon felt/*Ca*HydA electrodes were tested as the cathode in a photoelectrochemical biofuel cell. The short circuit photocurrent and rate of hydrogen production were comparable for either hydrogenase or platinum cathodes, indicating that hydrogenase is capable of maximizing the cell performance under the experimental conditions. This cell illustrates some of the limitations that must be overcome to carry out artificial photosynthesis that would ultimately involve water oxidation as the source of reducing equivalents and electroreductive chemistry at significantly negative potentials at the cathode.

Acknowledgment. We thank Dr. Anne K. Jones for helpful discussions and advice. We thank the U.S. Department of Energy (Grant No. DE-FG02-03ER15393) for supporting this work.

Supporting Information Available: Extensive experimental methods, additional cyclic voltammograms of platinum and *Ca*HydA modified carbon electrodes, and details of photocurrent and hydrogen production measurements in the photoelectrochemical cell. This material is available free of charge via the Internet at http://pubs.acs.org.

JA077691K